ACS APPLIED MATERIALS & INTERFACES

Research Article

www.acsami.org

M13 Bacteriophage Displaying DOPA on Surfaces: Fabrication of Various Nanostructured Inorganic Materials without Time-Consuming Screening Processes

Joseph P. Park,[†,§] Minjae Do,[‡,§] Hyo-Eon Jin,[∥,⊥] Seung-Wuk Lee,*[,∥,⊥] and Haeshin Lee*[,†,‡,§]

[†]The Graduate School of Nanoscience and Technology and [‡]Department of Chemistry, Korea Advanced Institute of Science and Technology (KAIST), Daejeon, South Korea

[§]Center for Nature-inspired Technology (CNiT) in KAIST institute NanoCentury, Korea Advanced Institute of Science and Technology (KAIST), Daejeon, South Korea

[∥]Department of Bioengineering, University of California, Berkeley, California 94720, United States

[⊥]Physical Biosciences Division, Lawrence Berkeley National Laboratory, Berkeley, California 94720, United States

Supporting Information

ABSTRACT: M13 bacteriophage (phage) was engineered for the use as a versatile template for preparing various nanostructured materials via genetic engineering coupled to enzymatic chemical conversions. First, we engineered the M13 phage to display TyrGluGluGlu (YEEE) on the pVIII coat protein and then enzymatically converted the Tyr residue to 3,4-dihydroxyl-L-phenylalanine (DOPA). The DOPA-displayed M13 phage could perform two functions: assembly and nucleation. The engineered phage assembles various noble metals, metal oxides, and semiconducting nanoparticles into one-dimensional arrays. Furthermore, the DOPA-displayed phage triggered the nucleation and growth of gold, silver, platinum, bimetallic cobalt–platinum, and bimetallic iron–platinum nanowires. This versatile phage template enables rapid preparation of phage-based prototype devices by eliminating the screening process, thus reducing effort and time.

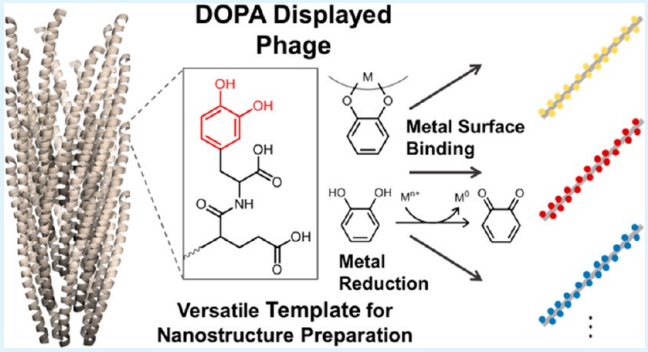

KEYWORDS: *bacteriophage, catechol, bioreduction, nanostructures, adhesion*

INTRODUCTION

Engineered viral particles have been used as templates to fabricate various nanostructures through genetic engineering, and these phage-templated functional nanomaterials are used in various devices for semiconductor, energy, biosensors, and biomedicine.[1−5] Specifically, the M13 bacteriophage (phage) is a filamentous-shape bacterial virus that contains a single stranded DNA encapsulated by 2700 copies of the pVIII coat protein, which is 880 nm in length and 6.6 nm in diameter.[6] This phage has been used extensively as a biological template because it can be easily engineered via genetic engineering or chemical conjugation to acquire various functionalities, such as specific material binding and nucleation capabilities.[6,7] To introduce new binding or nucleation functions to the M13 phage, a specific peptide motif must be identified via a time-consuming, multistep biopanning process.[8] So far, various inorganic nanostructures have been prepared using engineered M13 bacteriophages, and representative examples are shown in Table 1.

After screening, a peptide that exhibits the specific functionality is genetically incorporated into the M13 bacteriophage. The engineered phage is then used to align or nucleate nanoparticles. For example, a gold binding peptide, VSGSSPDS, was screened for and displayed on the pVIII proteins of the M13 phage to direct one-dimensional gold nanoparticle array formation.[11] Similarly, magnetic and semiconducting nanowires have been prepared by screening and displaying peptides with magnetic material binding affinities (HNKHLPSTQPLA and CNAGDHANC) and semiconductor binding affinities (CNNPMHQNC and SLTPLTTSHLRS).[18] The inorganic nanostructures templated by the engineered M13 phage have been used in applications, such as photovoltaics,[21] energy devices,[5,22−24] biosensors,[25] tissue engineering,[26] and medical imaging.[27] To engineer the M13 phage for the specific materials, it requires to invest effort to go through biopanning and further optimization of the time-demanding characterization. Furthermore, nanoparticle composites templated by engineered M13 phage such as CoPt and FePt have

Received: June 16, 2014
Accepted: October 15, 2014
Published: October 15, 2014

Table 1. M13 Phage-Based Inorganic Nanomaterials through Peptide Engineering

peptide sequence	inorganic material	function	ref
LKAHLPPSRLPS	Au	Au NP assembly	5
AHHAHHAAD	Au	Au nucleation	9, 10
VSGSSPDS	Au	Au specific binding peptide	11
AYSSGAPPMPPF	Ag	Ag NP synthesis	12
EEEE	Ag	Ag nucleation	13
PTSTGQA	Pt	Pt specific binding peptide	14
CPTSTGQAC (cyclic form)			
LSTVQTISPSNH	IONP	iron oxide binding peptide	15
CNNPMHQNC, QNPIHTH CTYSRLHLC	ZnS, PbS, CdS	semiconductor NP (Qdots) binding Peptide	16–18
HNKHLPSTQPLA SVSGMKPSPRP VISNHRESSRPL	FePt	FePt specific binding peptide	18, 19
CNAGDHANC	CoPt	CoPt specific binding peptide	18, 19
HYPTLPLGSSTY	CoPt	CoPt specific binding peptide	20

been reported,[18−24] in most cases, single inorganic material is templated by a single engineered M13 phage. Thus, it would be advantageous if a single engineered M13 phage could template a wide variety of nanostructured inorganic materials.

To develop a versatile phage that templates diverse material syntheses, 3,4-dihydroxyl-L-phenylalanine (DOPA), a key chemical component in the water-resistant adhesion of mussels, was introduced to the M13 phage surface. The DOPA-displayed phage may exhibit versatile template functionality and bind or nucleate a wide array of inorganic nanomaterials because catechol, the side chain of DOPA, strongly interacts with various organic and inorganic substrates through coordination, covalent bonds, $\pi-\pi$ stacking, electrostatic forces, and hydrogen bonding.[28,29] Furthermore, the catechol moiety possesses a significant redox activity that can chemically reduce metal ions. Catechol moieties can reduce gold and silver because they release electrons and oxidize into catechol quinone.[29−31] In this study, we report a mussel-inspired, DOPA-displayed M13 phage that not only assembles a wide array of inorganic nanoparticles but also nucleates various inorganic materials via the adhesive and redox properties of catechol without requiring a conventional biopanning process (Scheme 1).

EXPERIMENTAL DETAILS

M13 phage Engineering. The inverse polymerase chain reaction (PCR) cloning method was adapted to engineer the M13 phage major coat protein (pVIII).[32] Two primers were designed to insert YEEE into the pVIII coat protein: 5′-ATATATCTGCAGNKTAYGAAGAG-GA ANNKGATCCCGCAAAAGCGGCCTTTAACTCCC-3′ and 5′-GGAAGCTGCAGCGAAA GACAGCATCGGAACGAGG-3′. To engineer the YEEE phage (M13-YEEE8), a PCR reaction was performed using the above primers and the M13KE phage vector (New England Biolabs) as a template. The obtained PCR product was purified, treated with *Pst*I restriction enzyme (NEBiolabs), and recircularized via the overnight ligation at 16 °C using T4 DNA ligase (NEBiolabs). The ligated DNA vector was transformed into XL1-Blue electroporation competent cells (Stratagene) that were plated onto an LB agar plate containing IPTG and X-GAL after mixing with a top agar. The amplified plasmid and phage plaques were verified by DNA sequencing at the University of California, Berkeley DNA sequencing facility (Berkeley, CA).

Phage Amplification and Purification. To amplify the YEEE phage for further experiments, a XL1-Blue culture was grown overnight with the YEEE phage stock solution. After the overnight culturing, *E. coli* cells were removed from the culture via centrifugation at 8000 rpm for 20 min. The supernatant was collected, and a 20% PEG/2.5 M NaCl solution was added and incubated overnight at 4 °C to precipitate the phage. The precipitated phage was centrifuged and resuspended in 10 mM phosphate buffer (pH 5.8) for further experiments. The obtained phage solution was quantified using UV−vis spectrometry as previously reported.[33]

Conversion of tyrosine to DOPA residue. Tyrosinase from mushroom (Sigma-Aldrich) was used to convert the tyrosine residue of the engineered M13 phage (YEEE phage) into DOPA throughout these experiments. The tyrosinase was dissolved in distilled water to a concentration of 500 U/mL, where one unit represents a ΔA280 of 0.001 per min at a pH of 6.5 and 25 °C in a 3 mL reaction mixture containing L-tyrosine. The phage solution was treated with tyrosinase (500 U/mL) overnight at room temperature. After this tyrosinase treatment, the engineered phage was dialyzed against a 10 mM phosphate buffer (pH 5.8) using a cellulose/ester membrane (MWCO 300 kDa) to remove the tyrosinase enzyme and prevent any oxidation of the converted DOPA moiety.

NBT/Glycinate Assay. A NBT/glycinate assay was performed to confirm the tyrosine residue modification using previously reported method.[34] Two microliters of a 3 mg/mL YEEE phage solution and tyrosinase treated YEEE phage solution was dropped onto a polyvinylidene fluoride (PVDF) membrane (Millipore) until the solution had dried. The membrane was then incubated in a NBT/glycinate solution (0.6 mg/mL NBT in 2 M potassium glycinate buffer, pH 10) at room temperature until the color had developed. The stained membrane was then washed using a 0.1 M sodium borate solution and deionized water.

MALDI-ToF MS Analysis of the M13 pVIII Subunit. A MALDI-ToF analysis was performed to confirm the expression of the YEEE phage and tyrosine residue conversion into DOPA on the phage coat protein. A solution of the engineered M13 phages (1 mg/mL, 26 ul) was treated with 6 M guanidine-HCl (4 ul) for 5 min at room temperature. The denatured protein was spotted onto the MALDI sample plate using a Millipore ZipTip to remove the salts. The samples were analyzed using a Voyager mass spectrometer with sinapinic acid in 70% acetonitrile and 0.1% TFA as the matrix.

Analysis of DOPA Conversion Efficiency. To determine the tyrosinase conversion efficiency, we employed two different UV spectroscopic methods. First, UV spectroscopic method that determines the DOPA content by the formed catechol-borate complexes was employed.[35,36] The absorbance of DOPA-EEE phage in 0.2 N HCl and 0.2 M sodium borate buffer were scanned at 250−350 nm using a UV−visible spectrophotometer. The spectral difference was calculated by subtracting the spectra of DOPA-EEE phage in 0.2 N HCl from that obtained from the DOPA-EEE phage in 0.2 M sodium borate buffer. As a standard, 1 mM DOPA standard was used and the spectral difference was obtained using the same method. The 1 mM DOPA standard showed a subtraction difference λmax of 292 nm with a $\Delta\varepsilon$ value of 3200 M^{-1} cm^{-1}. Using the λmax and $\Delta\varepsilon$, the number of DOPA residues in the DOPA-EEE phages was calculated according to Beer's law. As another method to quantify the converted DOPA moiety, modified NBT/Glycinate assay was employed.[37] Twenty microliters of DOPA-EEE phage was incubated with 180 μL of NBT/Glycinate (0.2 mg NBT in 2 M glycinate buffer, pH 10) in 96-well plates at 25 °C in the dark for 1 h. After 1 h incubation, the absorbance at 530 nm was measured using UV−visible spectrophotometer. Standard curve was made using different concentrations of DOPA ranging from 0.002 to 0.02 μg incubated with NBT/Glycinate solution. The amount DOPA moiety present in DOPA-EEE phage was then calculated using the standard curve.

Assembly of Various Nanoparticles on Phage Template. Gold nanoparticles (5 nm, Sigma-Aldrich), Iron oxide nanoparticles (Fe_3O_4, 10 nm, Sigma-Aldrich), and quantum dots (Qdot, Invitrogen)

Scheme 1. Schematic Illustration of (A) Various Nanostructures Templated by the DOPA Displayed Phage and (B) Conventional Method for Preparing Engineered M13 Phage Templated Nanostructures[a]

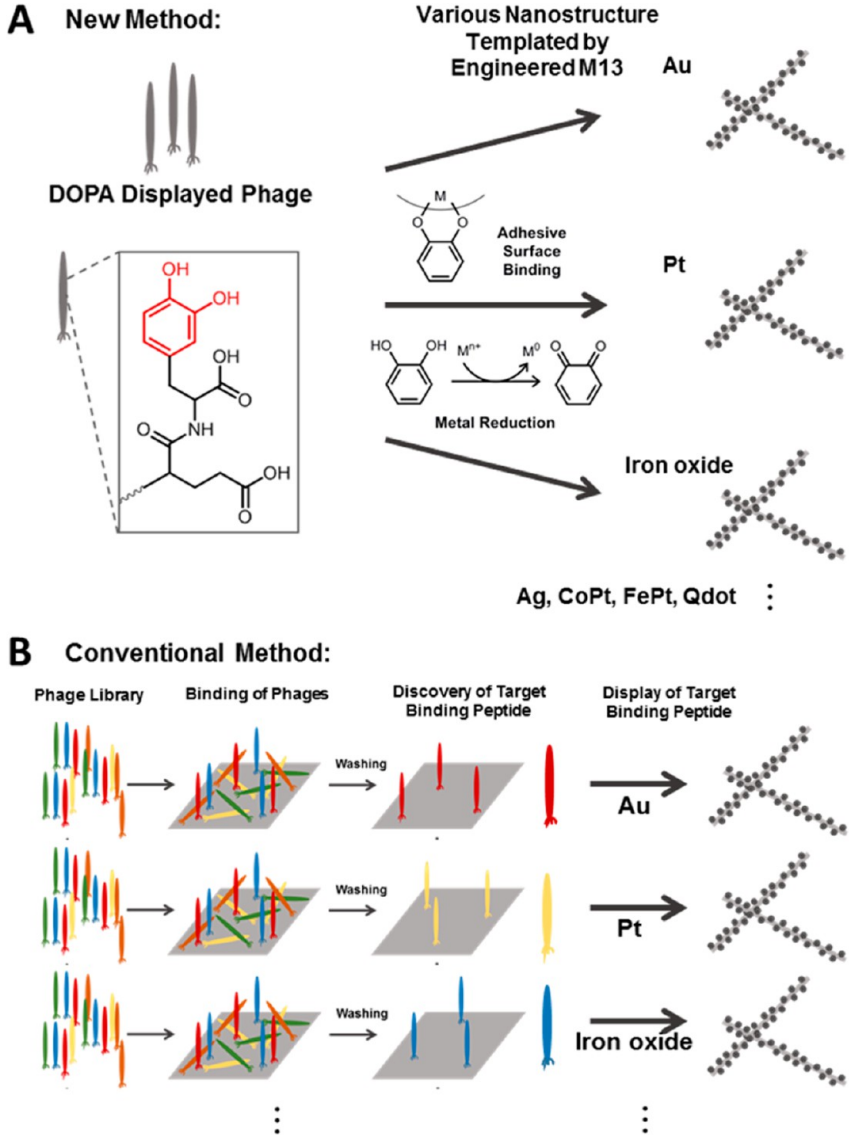

[a]Various nanostructures can be prepared using the adhesive surface binding and metal reduction of catechol moieties displayed on engineered M13 bacteriophage.

were used during the nanoparticle assembly experiments. The phage solution (0.5 mg/mL) was mixed and incubated with various nanoparticles for 4 h. After a 4 h incubation, the samples were analyzed via transmission electron microscopy (TEM).

Nanowire Synthesis Using Engineered Phage. To synthesize the noble metal nanowires, a phage solution (0.5 mg/mL) was mixed and incubated with 5 mM $HAuCl_4$, 5 mM $AgNO_3$, and 5 mM H_2PtCl_6 (Sigma-Aldrich) for 4 h. The CoPt and FePt alloy nanowires were prepared using a previously reported method.[18] The engineered phage template CoPt nanowire was synthesized by mixing 1 mL of the engineered phage (1 mg/mL) with 0.5 mM $CoCl_2$ and 0.5 mM H_2PtCl_6. For the FePt nanowire, 1 mL of the engineered phage (1 mg/mL) was mixed with 0.01 mM $FeCl_2$ and 0.01 mM H_2PtCl_6. These mixtures were vortexed for 10 min and 0.1 M $NaBH_4$ was added to the reaction mixture to reduce the metals into the desired nanowires. Sample preparation for TEM analysis: A reaction solution of the engineered M13 phages with various nanoparticles and metal solutions were deposited onto a 200-mesh carbon-coated copper grid for 3 min. After the 3 min of incubation, the reaction solutions were wicked from the TEM grid, which was washed once with deionized water. The grids were then stained with 2% uranyl acetate before the TEM analysis.

RESULTS AND DISCUSSION

To engineer 3,4-dihydroxyl-L-phenylalanine (DOPA) displayed M13 bacteriophage, a phage with a YEEE peptide on the N-terminus of the pVIII coat protein (termed YEEE phage) was engineered to induce a tyrosine, a tyrosinase substrate. The three-glutamate (EEE) moiety was designed to attract metal ions. An M13 phage displaying the YEEE sequence on the pVIII surface proteins was genetically engineered using recombinant DNA techniques. The sequence and location of the YEEE phage was confirmed via DNA sequencing. After confirming its successful engineering, the YEEE phage was treated with tyrosinase to convert the tyrosine residue to DOPA and obtain the DOPA-EEE phage (Figure 1). The successful conversion of tyrosine into DOPA was first investigated using a nitroblue tetrazolium (NBT) and glycinate

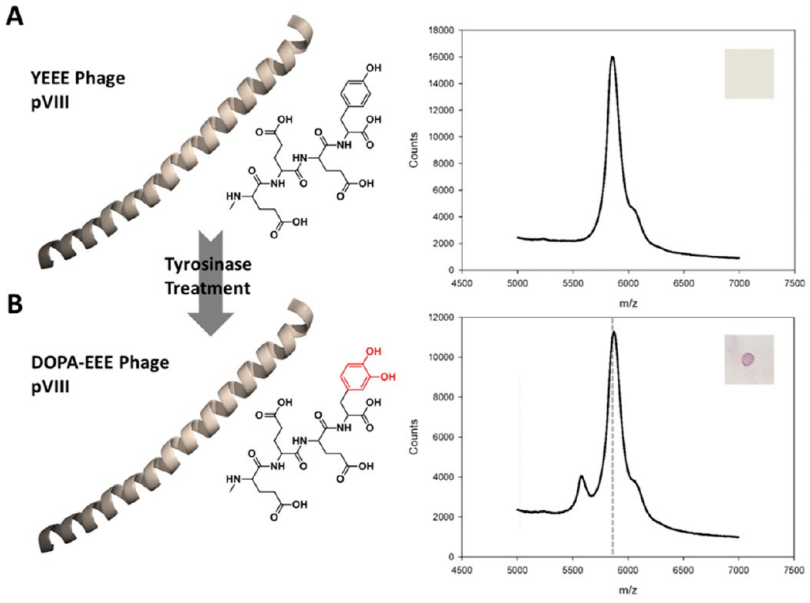

Figure 1. Confirmation of successful engineering YEEE and DOPA-EEE phages MADLI-ToF analysis and NBT/glycinate assay were performed on the (A) YEEE and (B) DOPA-EEE phages. After the tyrosinase treatment, the tyrosine residue of the YEEE phage is oxidized into the catechol-containing DOPA-EEE phage.

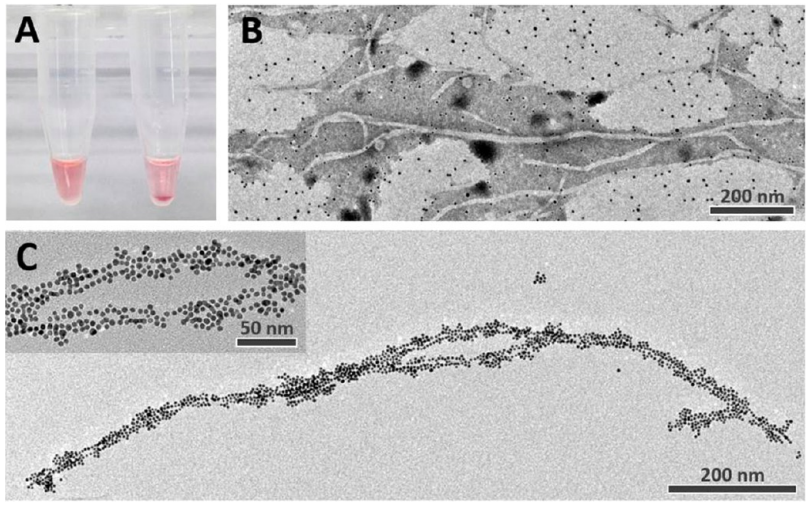

Figure 2. Gold NP Binding of DOPA-EEE phage. (A) Photograph of the YEEE (left) and DOPA-EEE (right) phages incubated with 5 nm AuNP. The incubated DOPA-EEE phage solution showed a visible precipitate, which indicates an interaction between the AuNP and the phages, whereas the YEEE phage solution remained clear. (B) TEM image of the YEEE phage incubated with AuNP (control) and stained with 2% uranyl acetate. No interactions between the YEEE phage and AuNPs were observed. (C) TEM images of the DOPA-EEE phage incubated with the AuNP. The AuNP particles assembled into 1D arrays only when incubated with the DOPA-EEE phage.

assay.[34] Proteins containing quinones and related quinonoids, such as dopaquinone and DOPA, are specifically stained by the NBT and glycinate solution as a result of their redox-cycling. The YEEE and DOPA-EEE phage solutions were dropped onto a nitrocellulose membrane and stained using the NBT/glycinate solution. While the YEEE phage was unstained, blue-purple spots were clearly observed for the DOPA-EEE phage as shown in Figure 1, which indicates the tyrosine was successful modified into DOPA. The successful conversion of tyrosine to DOPA was also confirmed via matrix-assisted laser desorption ionization-time-of-flight mass spectrometry (MALDI-ToF MS) of the pVIII coat protein. The molecular weight of the pVIII coat protein calculated for the YEEE phage was 5858.73. The MALDI-ToF MS analysis of the YEEE phage pVIII coat protein yielded a molecular weight of m/z 5858, which agrees with the calculated value (Figure 1A). The MALDI-ToF MS analysis of the tyrosinase-treated YEEE phage (DOPA-EEE phage) pVIII coat protein yielded a molecular weight of m/z 5874, which corresponds to the oxidation of the tyrosine residue that confirms the successful conversion to DOPA (Figure 1B). The MALDI-ToF MS analysis of the pVIII protein and NBT/glycinate assay provide sufficient evidence that the YEEE and DOPA-EEE phages were successfully engineered.

To quantify the proportion of tyrosine residue modified to DOPA, we employed two different UV−vis spectroscopy based analysis: (1) catechol-borate complex formation and (2) modified NBT/glycinate assay. The DOPA conversion determined by catechol-borate complexation method was calculated to be 61.4%. Similarly, the conversion efficiency

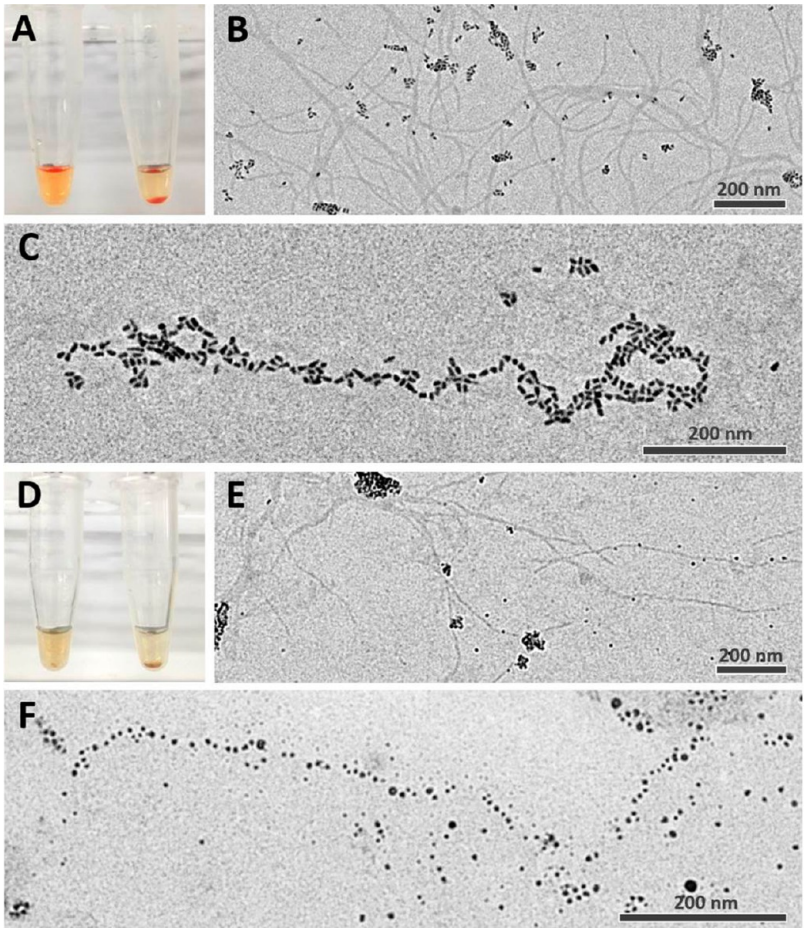

Figure 3. IONP and QD Binding of DOPA-EEE phage. (A, D) Photograph of the YEEE (left) and DOPA-EEE (right) phages incubated with 15 nm QD and 10 nm IONP, respectively. The DOPA-EEE phage solution yielded a visible precipitate, which indicates an interaction between the nanoparticles and the phages, whereas the YEEE phage incubated solution remained clear. B and E) TEM image of the YEEE phage incubated with QD and IONP (control) and stained with 2% uranyl acetate. No interactions between the YEEE phage and the AuNP were observed. (C, F) TEM images of DOPA-EEE phage incubated with QD and IONP. The nanoparticles only assembled into 1D arrays when incubated with the DOPA-EEE phage.

measured by the NBT/glycinate assay exhibited DOPA conversion of 55.6%. However, the actual conversion rate from tyrosine to DOPA might be higher than the measured two values since the analytical methods cannot detect the oxidized species called catecholquinone, which might in part be presented on the phage surface. After confirming the successful engineering of the DOPA-EEE phage, its capabilities as a nanoparticle assembly template were investigated. The catechol moiety, which is a side chain of the displayed DOPA, is known to play a key role in the water-resistant adhesion of mussels, and studies show that it strongly interacts with a variety of organic and inorganic substrates via various means such as coordination, covalent bonds, electrostatic forces, hydrogen bonding and $\pi-\pi$ stacking.[28,29] To prove that the DOPA-EEE phage can be used as a nanoparticle assembly template, it was tested with gold nanoparticles (5 nm). The YEEE and DOPA-EEE phages were incubated with gold nanoparticles for 4 h, and their morphologies were observed via transmission electron microscopy (TEM). In the TEM images, the DOPA-EEE phage exhibited the one-dimensional assembly of gold nanoparticles into wire-like structures along the M13 virus outline (Figure 2C). By contrast, the gold nanoparticles were randomly distributed for the YEEE phage with no interactions as shown in Figure 2B. A visible precipitate was also observed in the DOPA-EEE phage-gold nanoparticle solution, whereas the YEEE phage-gold nanoparticle solution remained clear (Figure 2A) after incubating overnight.

To demonstrate that the DOPA-EEE phage can be used to assemble various nanoparticles, two widely used nanoparticles, quantum dots (QD, 15 nm) and iron oxide nanoparticles (IONP, 10 nm), were also used. The DOPA-EEE phage interacted with both the IONP and QD as shown in Figure 3. The QD and IONP all aligned along the viral axis of the DOPA-EEE phage to form anisotropic, linear nanoparticle chains (Figure 3C, F), whereas no interactions were observed for the YEEE phage (Figure 3B, E). Precipitation was again observed for the DOPA-EEE phage nanoparticle solution after incubating overnight but not for the YEEE phage, which indirectly confirms the nanoparticle interactions (Figure 3A, D). The DOPA-EEE phage successfully templated three widely used representative nanoparticles—a metal oxide, semiconductor, and noble metal nanoparticle—and demonstrated its versatility as a 1D assembly template.

Next, the ability of the DOPA-EEE phage to nucleate and grow nanoparticles on its surface was investigated. Catechol moieties are known to possess a certain redox activity. When the catechol moiety oxidizes into catecholquinone, it releases electrons and spontaneously reduces various metal ions.[29−31]

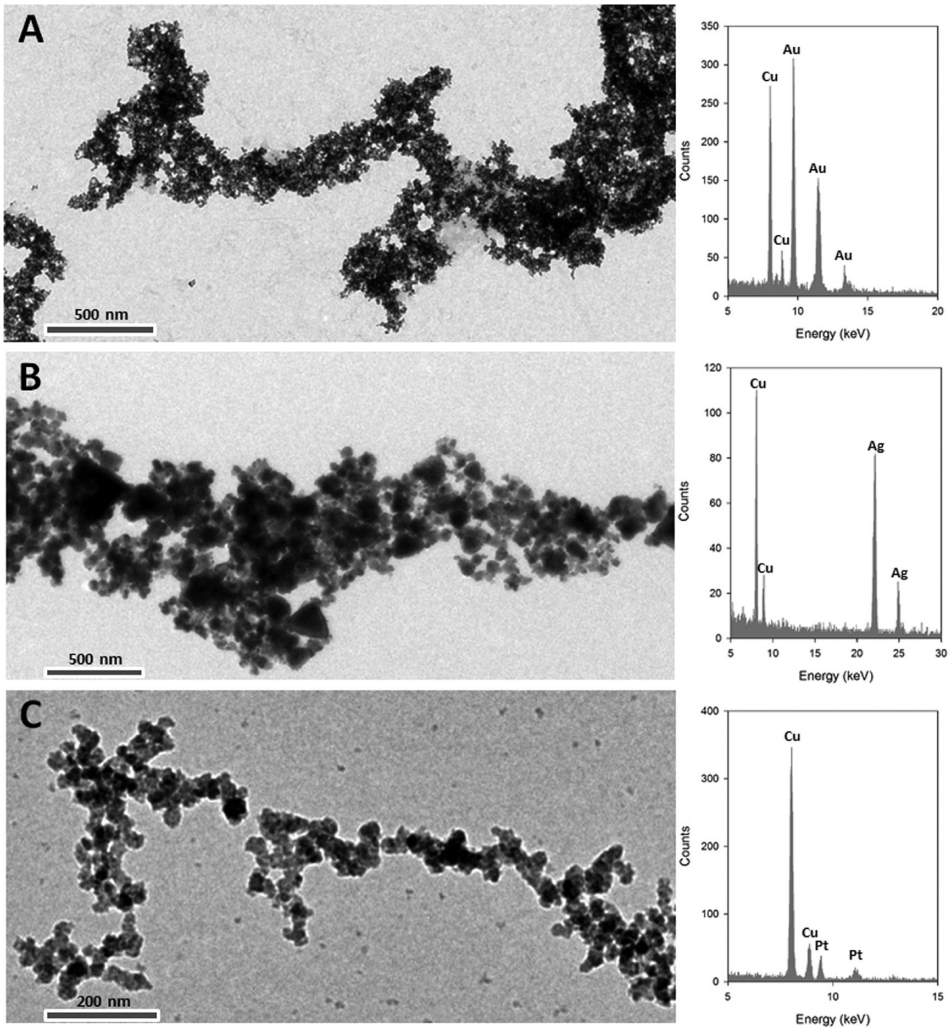

Figure 4. Treelike nanowires synthesized using the DOPA-EEE phage. TEM images of (A) gold, (B) silver, (C) platinum nanowires synthesized using the DOPA-EEE phage as a template. The TEM EDS spectra are present on the right for each nanowires, which confirms their composition.

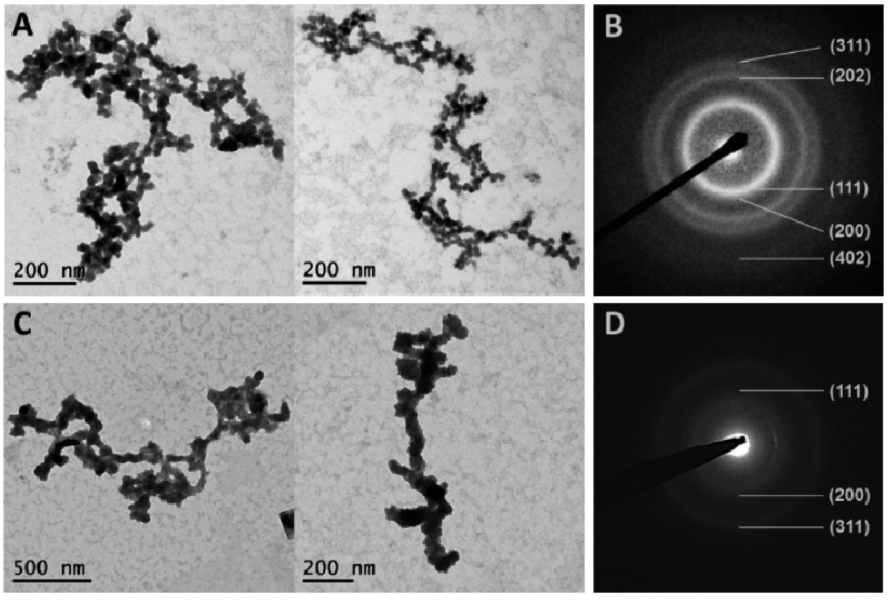

Figure 5. Bimetallic Pt alloy nanowires synthesized using DOPA-EEE phage. TEM image of the (A) CoPt and (C) FePt synthesized using DOPA-EEE as a template. (B, D) SAED patterns for the corresponding nanowires.

Therefore, the DOPA-EEE phage is expected to reduce noble metal ions owing to the reductive properties of catechol. DOPA-EEE phages and YEEE phages were incubated with various noble metal salt solutions, $HAuCl_4$, $AgNO_3$, and H_2PtCl_6. The morphology of the phages were then observed via TEM. Both gold and platinum were reduced on the DOPA-EEE phage into tree-like nanowire structures as shown in Figure 4, whereas, no nanowirelike structures were observed when the YEEE phage was incubated with $HAuCl_4$ and H_2PtCl_6 (see Figure S1 in the Supporting Information). For the engineered phages incubated with $AgNO_3$ solution, the silver was reduced to form treelike nanowire structures on both the DOPA-EEE and YEEE phage surfaces. The reduction of silver on both of the engineered phages can be explained by the common "EEE" moiety, which is previously known to reduce and nucleate silver as a result of the high surface charge density.[13] Energy-dispersive X-ray spectroscopy (EDS) was used to confirm the nanowire composition, and all of the EDS results corresponded to the anticipated material (Figure 4). After confirming noble metals could be reduced on the DOPA-EEE phage surface, the engineered phages were incubated with cobalt or iron with platinum to test their ability to template and synthesize metal alloy nanowires. After synthesizing the CoPt and FePt nanowires using the DOPA-EEE phage template via the previously reported methods,[18] the nanowire morphologies were determined via TEM. A nanowirelike morphology was observed for the DOPA-EEE phage incubated with both bimetallic salt solutions (Co and Pt, Fe, and Pt), which confirms the successful nucleation of the CoPt and FePt particles at the engineered M13 phage surface (Figure 5).

The corresponding selected area electron diffraction (SAED) patterns for the obtained CoPt and FePt nanowires were also observed and confirmed the successful alloy metal nanowire formation. The SAED patterns for the M13 CoPt alloy nanowire (Figure 5B) showed the ring pattern for the face-centered cubic (FCC) CoPt phase[38] with diffuse continuous ring, which indicates the polycrystalline nature of the alloy. The SAED pattern for the FePt alloy nanowire (Figure 5D) confirmed the distorted face-centered cubic (DFCC) FePt phase with [1,1,1] and [2,0,0] faces, which agrees with previously reported SAED patterns for FePt alloys.[39] Both metal alloy nanowires exhibited low crystallinity; however, the crystallinity was not enhanced via high temperature annealing because this study is a proof of concept for using the DOPA-EEE phage as a template to synthesize metal alloy nanowires. By contrast, no nanowire-like morphology was observed when the YEEE phages were incubated with the bimetallic salt solutions (see Figure S2 in the Supporting Information).

In this study, we demonstrated that a single engineered DOPA-EEE M13 phage can act as a versatile nanoscale biological template for the assembly and nucleation of all the materials listed in Table 1: Au, Ag, Pt, IONP, CdS, FePt, and CoPt. So far, conventional studies have used screened peptides that bind or nucleate a specific material to prepare inorganic nanostructures. Using a nonspecific peptide interaction with various materials can be an alternative approach toward engineered phages with multiple targets. One example is the engineered tetraglutamate (EEEE) displayed phage, which was used to prepare Ag nanowires.[13] Later, it was found that the EEEE displayed phage is capable of nonspecifically interacting with cobalt,[5] and iron phosphate.[22] EEEE phages have high charge densities and increased ionic interactions with cations due to the presence of carboxyl groups on their surface, which enables metals nucleation.[13] However, the EEEE sequence only utilizes electrostatic binding, which intrinsically lacks material versatility and has a weak binding strength. By contrast, incorporating catechol (i.e., DOPA) into the peptide sequence provides a dramatically different result. As previously mentioned, catechol utilizes several binding mechanisms, such as coordination, $\pi-\pi$ stacking, covalent, and electrostatic force. Furthermore, the redox capabilities of catechol are an important advantage when preparing various metallic nanostructures. Though our DOPA displayed bacteriophage is a versatile template in preparing various nanostructures, there are limitations related to the tyrosine to DOPA conversion efficiency by the enzymatic action of tyrosinase. The conversion efficiency determined by the UV spectrometric methods, catechol–borate complex and modified NBT/glycinate assay, revealed that about 60% of tyrosine was converted to DOPA. However, the 60% DOPA conversion was sufficient to anchor nanoparticles and reduce metal ions on M13 phage surfaces. Unnatural amino acids such as DOPA can also be genetically incorporated onto the M13 bacteriophage surface using engineered tRNA and aminoacyl-tRNA synthases which may increase the DOPA content of the DOPA-EEE phage but the process may be more energy and time-consuming.[40,41]

CONCLUSION

In conclusion, we have shown the versatility of the DOPA engineered M13 phage to assemble and reduce a variety of inorganic material via the unique properties of the catechol moieties displayed on the major coat surface. The nonspecific binding capabilities and redox properties of catechol can make the DOPA incorporated M13 phage a powerful template for various inorganic nanostructures.

ASSOCIATED CONTENT

Supporting Information

TEM analysis of YEEE phage incubated with Au and Pt metal solution, and TEM analysis of CoPt and FePt nanowires synthesized using YEEE and DOPA-EEE phage. This material is available free of charge via the Internet at http://pubs.acs.org.

AUTHOR INFORMATION

Corresponding Authors

*E-mail: haeshin@kaist.ac.kr.
*E-mail: leesw@berkeley.edu.

Notes

The authors declare no competing financial interest.

ACKNOWLEDGMENTS

This work was supported by the National Research Foundation of Korea (NRF): Midcareer scientist grant (2014002855, H.L.) and Basic Science Research Program (2011-357-E00083, H.E.J.). This work is in part supported by the Ministry of Health and Welfare of Korea (A120170, H.L.). SWL was supported by the National Science Foundation Early Career Development Award (DMR-0747713) and the Center of Integrated Nanomechanical Systems (COINS) of the National Science Foundation (Grant EEC-0832819).

REFERENCES

(1) Lucon, J.; Qazi, S.; Uchida, M.; Bledwell, G.; LaFrance, B.; Prevelige, P.; Douglas, T. Using the Interior of the P22 Capsid for Site Specific Initiation of Atom Transfer Radical Polymerization with

Tremendously Increased Cargo Loading. *Nat. Chem.* **2012**, *4*, 781−788.
(2) Chung, W. J.; Oh, J.-W.; Kwak, K.-W.; Lee, B.-Y.; Mayer, J.; Wang, E.; Hexemer, A.; Lee, S.-W. Biomimetic Self-Templating Supramolecular Structures. *Nature* **2011**, *478*, 364−368.
(3) Lee, B.-Y.; Zheng, J.; Zueger, C.; Chung, W.-J.; Yoo, S.-Y.; Wang, E.; Meyer, J.; Ramesh, R.; Lee, S.-W. Virus-Based Piezoelectric Energy Generation. *Nat. Nanotechnol.* **2012**, *7*, 351−356.
(4) Oh, J.-W.; Chung, W.-J.; Heo, K.; Jin, H.-E.; Lee, B.-Y.; Wang, E.; Meyer, J.; Kim, C.; Lee, S.-Y.; Kim, W.-G.; Zemla, M.; Auer, M.; Hexemer, A.; Lee, S.-W. Biomimetic Virus-Based Colourimetric Sensors. *Nat. Commun.* **2014**, *5*, 3043.
(5) Nam, K. T.; Kim, D. W.; Yoo, P. J.; Chiang, C. Y.; Meethong, N.; Hammond, P. T.; Chiang, Y. M.; Belcher, A. M. Virus-Enabled Synthesis and Assembly of Nanowires for Lithium Ion Battery Electrodes. *Science* **2006**, *312*, 885−888.
(6) Smith, G. P.; Petrenko, V. A. Phage Display. *Chem. Rev.* **1997**, *97*, 391−410.
(7) Yang, S. H.; Chung, W.-J.; McFarland, S.; Lee, S.-W. Assembly of Bacteriophage into Functional Materials. *Chem. Rec.* **2013**, *13*, 43−59.
(8) Seeman, N. C.; Belcher, A. M. Emulating Biology: Building Nanostructures from the Bottom Up. *Proc. Natl. Acad. Sci. U.S.A.* **2002**, *99*, 6451−6455.
(9) Slocik, J. M.; Moore, J. T.; Wright, D. W. Monoclonal Antibody Recognition of Histidine-Rich Peptide Encapsulated Nanoclusters. *Nano Lett.* **2002**, *2*, 169−173.
(10) Djalali, R.; Chen, Y.-F.; Matsui, H. Au Nanocrystal Growth on Nanotubes Controlled by Conformations and Charges of Sequenced Peptide Templates. *J. Am. Chem. Soc.* **2003**, *125*, 5873−5879.
(11) Huang, Y.; Chiang, C. Y.; Lee, S. K.; Gao, Y.; Hu, E. L.; De Yoreo, J.; Belcher, A. M. Programmable Assembly of Nanoarchitectures Using Genetically Engineered Viruses. *Nano Lett.* **2005**, *5*, 1429−1434.
(12) Naik, R. R.; Stringer, S. J.; Agarwal, G.; Jones, S. E.; Stone, M. O. Biomimetic Synthesis and Patterning of Silver Nanoparticles. *Nat. Mater.* **2002**, *1*, 169−172.
(13) Nam, K. T.; Lee, Y. J.; Karuland, E. M.; Kottmann, S. T.; Belcher, A. M. Peptide-Mediated Reduction of Silver Ions on Engineered Biological Scaffolds. *ACS Nano* **2008**, *2*, 1480−1486.
(14) Seker, U. O.; Wilson, B.; Dincer, S.; Kim, I. W.; Oren, E. E.; Evans, J. S.; Tamerler, C.; Sarikaya, M. Adsorption Behavior of Linear and Cyclic Genetically Engineered Platinum Binding Peptides. *Langmuir* **2007**, *23*, 7895−7900.
(15) Lower, B. H.; Lins, R. D.; Oestreicher, Z.; Straatsma, T. P.; Hochella, M. F.; Shi, L. A.; Lower, S. K. In Vitro Evolution of Peptide with a Hematite Binding Motif That May Constitute a Natural Metal-Oxide Binding Archetype. *Environ. Sci. Technol.* **2008**, *42*, 3821−3827.
(16) Flynn, C. E.; Mao, C.; Hayhurst, A.; Wiliams, J. L.; Georgiou, G.; Iverson, B.; Belcher, A. M. Synthesis and Organization of Nanoscale II-VI Semiconductor Materials Using Evolved Peptide Specificity and Viral Capsid Assembly. *J. Mater. Chem.* **2003**, *13*, 2414−2421.
(17) Mao, C.; Flynn, C. E.; Hayhurst, A.; Sweeney, R. Y.; Qi, J.; Georgiou, G.; Iverson, B.; Belcher, A. M. Viral Assembly of Oriented Quantum Dot Nanowires. *Proc. Natl. Acad. Sci. U. S. A.* **2003**, *100*, 6946−6951.
(18) Mao, C.; Solis, D. J.; Reiss, B. D.; Kottmann, S. T.; Sweeney, R. Y.; Hayhurst, A.; Georgiou, G.; Iverson, B.; Belcher, A. M. Virus-Based Toolkit for the Directed Synthesis of Magnetic and Semiconducting Nanowires. *Science* **2004**, *303*, 213−217.
(19) Reiss, B. D.; Mao, C.; Solis, D. J.; Ryan, K. S.; Thomson, T.; Belcher, A. M. Biological Routes to Metal Alloy Ferromagnetic Nanostructures. *Nano Lett.* **2004**, *4*, 1127−1132.
(20) Naik, R. R.; Jones, S. E.; Murray, C. J.; McAuliffe, J. C.; Vaia, R. A.; Stone, M. O. Peptide Templates for Nanoparticles Synthesis Derived from Polymerase Chain Reaction-Driven Phage Display. *Adv. Funct. Mater.* **2004**, *14*, 25−30.
(21) Dang, X. N.; Yi, H. J.; Ham, M. H.; Qi, J.; Yun, D. S.; Ladewski, R.; Strano, M. S.; Hammond, P. T.; Belcher, A. M. Virus-Templated Self-Assembled Single-Walled Carbon Nanotubes for Highly Efficient Electron Collection in Photovoltaic Devices. *Nat. Nanotechnol.* **2011**, *6*, 377−384.
(22) Lee, Y. J.; Yi, H.; Kim, W. J.; Kang, K.; Yun, D. S.; Strano, M. S.; Ceder, G.; Belcher, A. M. Fabricating Genetically Engineered High-Power Lithium-Ion Batteries Using Multiple Virus Genes Science. *Science* **2009**, *324*, 1051−1055.
(23) Nam, Y. S.; Magyar, A. P.; Lee, D.; Kim, J.-W.; Yun, D. S.; Park, H.; Pollom, T. S., Jr.; Weitz, D. A.; Belcher, A. M. Biologically Template Photocatalytic Nanostructures for Sustained Light-Driven Water Oxidation. *Nat. Nanotechnol.* **2010**, *5*, 340−344.
(24) Lee, Y.; Kim, J.; Yun, D. S.; Nam, Y. S.; Shao-Horn, Y.; Belcher, A. M. Virus-Templated Au and Au-Pt Core-Shell Nanowires and Their Electrocatalytic Activities for Fuel Cell Applications. *Energy Environ. Sci.* **2012**, *5*, 8328−8344.
(25) Mao, C.; Liu, A.; Cao, B. Virus-based Chemical and Biological Sensing. *Angew. Chem., Int. Ed.* **2009**, *48*, 6790−6810.
(26) Rong, J.; Lee, L. A.; Li, K.; Harp, B.; Mellow, C. M.; Niu, Z.; Wang, Q. Oriented Cell Growth on Self-Assembled Bacteriophage M13 Thin Films. *Chem. Commun.* **2008**, 5185−5187.
(27) Ghosh, D.; Lee, Y.; Thomas, S.; Kohli, A. G.; Yun, D. S.; Belcher, A. M.; Kelly, K. A. M13-Templated Magnetic Nanoparticles for Targeted in Vivo Imaging of Prostate Cancer. *Nat. Nanotechnol.* **2012**, *7*, 677−682.
(28) Lee, H.; Scherer, N. F.; Messersmith, P. B. Single-Molecule Mechanics of Mussel Adhesion. *Proc. Natl. Acad. Sci. U.S.A.* **2006**, *103*, 12999−13003.
(29) Lee, H.; Dellatore, S. M.; Miller, W. M.; Messersmith, P. B. Mussel-Inspired Surface Chemistry for Multifunctional Coatings. *Science* **2007**, *318*, 426−430.
(30) Lee, Y.; Park, T. G. Facile Fabrication of Branched Gold Nanoparticles by Reductive Hydroxyphenol Derivatives. *Langmuir* **2011**, *27*, 2965−2971.
(31) Son, H. Y.; Ryu, J. H.; Lee, H.; Nam, Y. S. Silver-Polydopamine Hybrid Coatings of Electrospun Poly(vinyl alcohol) Nanofibers. *Macromol. Mater. Eng.* **2013**, *298*, 547−554.
(32) Merzlyak, A.; Indrakanti, S.; Lee, S.-W. Genetically Engineered Nanofiber-Like Viruses For Tissue Regenerating Materials. *Nano Lett.* **2009**, *9*, 846−852.
(33) Sambrook, J.; Rissell, D. W. *Molecular Cloning: A Laboratory Manual*, 3rd ed.; CSHL Press: Cold Spring Harbor, NY, 2001.
(34) Paz, M. A.; Flückiger, R.; Boak, A.; Kagan, H. M.; Gallop, P. M. Specific Detection of Quinoproteins by Redox-Cycling Staining. *J. Biol. Chem.* **1991**, *266*, 689−692.
(35) Waite, J. H. Determination of (catecholato)-borate complex using difference spectrometry. *Anal. Chem.* **1984**, *56*, 1935−1939.
(36) Hwang, D. S.; Gim, Y.; Yoo, H. J.; Cha, H. J. Practical recombinant hybrid mussel bioadhesive fp-151. *Biomaterials* **2007**, *28*, 3560−3568.
(37) Li, N.-N.; Shi, G.; Yang, X.-X.; Wang, Z.-P.; Liao, Z. Detection of Dihydroxyphenylalanine in Native Foot Proteins from Mytilus coruscus Byssus. *Chin. J. Biochem. Mol. Biol.* **2011**, *27*, 148−153.
(38) Huang, Y. H.; Zhang, Y.; Hadjipanayis, G. C.; Simopoulos, A.; Weller, D. Hysteresis Behavior of CoPt Nanoparticles. *IEEE Trans. Magn.* **2002**, *38*, 2604−2606.
(39) Medwal, R.; Sehdev, N.; Annapoorni, S. Order-Disorder Investigation of Hard Magnetic Nanostructured FePt Alloy. *J. Phys. D: Appl. Phys.* **2012**, *45*, 1−6.
(40) Moor, N.; Klipcan, L.; Safro, M. G. Bacterial and Eukaryotic Phenylalanyl-tRNA Synthetases Catalyze Misaminoacylation of tRNAPhe with 3,4-Dihydroxy-L-Phenylalanine. *Chem. Biol.* **2011**, *18*, 1221−1229.
(41) Tian, F.; Tsao, M.-L.; Schultz, P. G. A Phage Display System with Unnatural Amino Acids. *J. Am. Chem. Soc.* **2004**, *126*, 15962−15963.